Journal of Thermal Analysis and Calorimetry, Vol. 75 (2004) 975–988

PICOLINE AS LIGAND WITH ANTIMONY TRICHLORIDE AND TRIIODIDE ADDUCTS

F. M. L. Pontes [1], *S. F. Oliveira* [1], *J. G. P. Espínola* [1], *L. N. H. Arakaki* [1], *M. G. Fonseca* [1*] *and C. Airoldi* [2]

[1]Departamento de Química, CCEN, Universidade Federal da Paraíba, Caixa Postal 5093, 58059-900 João Pessoa, Paraíba, Brazil
[2]Instituto de Química, Universidade Estadual de Campinas, Caixa Postal 6154, 13084-971 Campinas, São Paulo, Brazil

Abstract

Solid adducts SbX_3·L-pic (*X*=Cl, I and *L*=α-, β- and γ-picolines) were synthesized and characterized by elemental analysis, ^1H and ^{13}C NMR, IR spectroscopy and thermal analysis. The infrared spectroscopy and the magnetic resonance for ^1H and ^{13}C nuclei of these compounds suggest that the ligands coordinate through nitrogen atom. Kinetic studies were accomplished by means of thermogravimetric data, through isothermal and non-isothermal techniques. The best adjusting models for adducts thermal decomposition were R_1 for isothermal and R_1 and R_2 for the non-isothermal methods. The energy of activation values obtained by isothermal method indicate the following orders of thermal stability for adducts: *i*) $SbCl_3$·α-pic>$SbCl_3$·β-pic>$SbCl_3$·γ-pic and *ii*) SbI_3·β-pic<SbI_3·γ-pic<SbI_3·α-pic. The activation energy values obtained by non-isothermal were higher than those from isothermal methods, showing the order of stability: *iii*) $SbCl_3$·α-pic<$SbCl_3$·β-pic<$SbCl_3$·γ-pic and *iv*) SbI_3·β-pic<SbI_3·α-pic≅SbI_3·γ-pic. These obtained data through R_1 model presented the kinetic compensation effect for trichloride adducts, which could be associated to both isothermal and non-isothermal processes.

Keywords: antimony halide, α-, β- and γ-picolines, kinetic

Introduction

Several investigations involving adducts of α-, β- and γ-picoline bases with transition metal salts have been reported [1–5], which main focus is based on synthetic and structural feature determinations, followed by some thermal decomposition process of such kind of compounds. A clear example of such behavior is illustrated with γ-picoline/cobalt halide complexes, in which the chloride adducts thermal study showed five distinct steps of decomposition, differing from seven stages observed for bromides and iodides. In all cases, a leaving residue of cobalt halide was detected with a decrease of stability following from chloride to iodide [1, 2].

* Author for correspondence: E-mail: gardennia@bol.com.br

1388–6150/2004/ $ 20.00

Akadémiai Kiadó, Budapest
Kluwer Academic Publishers, Dordrecht

The complete series of picolines, α-, β- and γ-forms, are potentially good bases to coordinate the similar acids arsenic, antimony and bismuth halides, however, fewer studies were devoted to such investigation [6, 7]. On the other hand, those elements forms vary stable bond with other metals, such as transition elements [4, 5]. From the energetic point of view, some parameters describe the strength of the main group element-base interaction, which results derived from decomposition of the adducts, as observed, for example, the mean arsenic-nitrogen bond formation in arsenic(III) compounds [6], and thermal decomposition of bismuth(III) compounds [7]. In spite of the reports concerned with adducts of antimony halides with other Lewis bases [8, 9], no other publication appeared with any form of this set of picolines. Adducts with molar ratio 1:1 are mentioned, however, the results seem to be simpler than those containing α-, β- and γ-picolines with transition metals [1–5].

Taking into account that antimony(III) halides have ability in coordinating α-, β- and γ-picolines through the available pair of electrons disposed on nitrogen atom of each base, as shown in Fig. 1, a typical Lewis acid–base reaction to form adducts is expected, being easier to form a 1:1 molar ratio compound, which presence of the methyl group attached to the cyclic ring can affect the basicity of the nitrogen atom used to bond the main element considered. Thus, the aim of this investigation is focusing on synthesis and characterization of antimony trichloride and iodide adducts with this complete set of picolines.

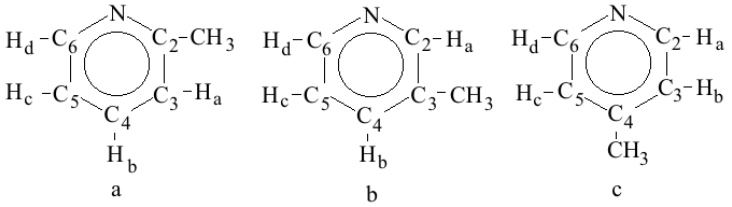

Fig. 1 Structural representation of picolines: a – α- ; b – β- and c – γ-forms

Experimental

Chemicals

The solvents used in all the preparations were distilled and stored over Linde 4 Å molecular sieve. Picolines (Merck) were used without further purification, and antimony trichloride (Merck) was dried in vacuum. All preparations and manipulations were performed under dryness condition in an inert atmosphere of nitrogen.

Preparations

Adducts were prepared by mixing equimolar amount of both reactants in carbon sulfide as solvent. Each individual preparation consisted in adding the correspondent liquid picoline to the stirred dissolved solution of SbX_3 (X=Cl and I) in the solvent chosen and the mixture was stirred for 3 h. After solvent removal, the formed solids

were washed with carbon sulfide and dried in vacuum. The yield for all the preparations was in the 80–90% range.

Physical measurements

Melting points of all the compounds were determined on Microquimica model MQAPF-301 apparatus. Infrared spectra in 4000–400 cm^{-1} range were obtained with a Bomen model MB-102 spectrophotometer, with the samples in Nujol emulsion. NMR (^{1}H and ^{13}C) spectra were recorded on a Varian Unity plus-300 with working frequency of 300 MHz, using deutered chloroform and hexadeutered dimethylsulfoxide as solvents and tetramethylsilane (TMS) as external reference. Thermogravimetric curves were obtained using a Shimadzu TG-50 thermobalance through isothermal and non-isothermal techniques. In the non-isothermal process experiments nitrogen flow rate of 50 $cm^3\ s^{-1}$, sample mass of 5.0±0.5 mg and heating rate of 1.67 K s^{-1} was used. The choice of temperatures for the isothermal process experiments was based on the curves for non-isothermal processes. The samples were submitted to granulometric control because the adducts decomposed at lower temperature than that of fusion, as it can be observed in Table 1. The non-isothermal kinetic parameters were determined by Coats–Redfern [10] method using a visual program developed in TAL (Thermal Analysis Laboratory). This visual basic program was also developed in the TAL for the isothermal method.

Results and discussion

Elemental analysis, thermal decomposition and infrared spectroscopy

Adducts of general formula SbX_3·L-pic for *X*=Cl and I were synthesized and studied by different spectroscopic methods. The elemental analysis results of the solid adducts are in complete agreement with this proposed general formula, as can be observed in Table 1.

The infrared spectra assignments were based on previous reports [11, 12]. The main vibrational absorptions for adducts are listed in Table 2 and some bands are shifted when compared with the correspondent free ligand spectra. However, the main characteristics of the bands of adducts are similar to those of the free ligands. This behavior can be explained due to the vibrations of ligands were not modified by geometry of adduct or halide.

The thermal decomposition of all adducts indicated that the trichloride compounds started to decompose at a lower temperature than the triiodide analogues. The thermogravimetric curves of adducts decomposition presented similar behavior, with a mass loss for a single step in the 99% range. Typical results are summarized for α-picoline SbI_3 adducts in Fig. 2. The same behavior was also observed for arsenic trichloride adducts [6], containing these three picolines. The well-defined melting points are given in Table 1, by including the interval of temperatures for the thermal decomposition processes.

Table 1 Analytical data, melting point (*MP*) temperature range of decomposition (ΔT) for adducts of antimony trichloride and triiodide with α-, β- and -picolines

Adduct	C/%	H/%	N/%	X/%	*MP*/K	ΔT/K
$SbCl_3$·α-pic	22.38 (21.8)	2.17 (2.1)	4.35 (4.3)	33.11 (33.5)	390	388–527
$SbCl_3$·β-pic	22.38 (22.8)	2.17 (2.0)	4.35 (4.4)	33.11 (33.4)	421	392–515
$SbCl_3$·γ-pic	22.38 (21.7)	2.17 (2.1)	4.35 (4.3)	33.11 (32.8)	464	410–501
SbI_3·α-pic	12.08 (12.0)	2.17 (2.1)	2.35 (2.3)	63.92 (64.0)	443	417–539
SbI_3·β-pic	12.08 (12.0)	1.18 (1.2)	2.35 (2.4)	63.92 (63.9)	449	417–559
SbI_3·γ-pic	12.08 (12.1)	1.18 (1.2)	2.35 (2.4)	63.92 (63.9)	456	416–554

Table 2 Infrared data for adducts and α-, β- and γ-picolines

Compound	ν_{CC}	$\nu_{CC,CN}$	$\nu_{CC,CN}$	δ_{CH}	X-sens	β_{CH}	ϕ_{CH}
α-pic	1594s	1478s	1377w	1295m	1101w	1150m	754s
$SbCl_3$·α-pic	1543s	1472w	no	no	no	1256w	1183w
SbI_3·α-pic	1532m	1461w	no	1384w	1277w	1232w	165w
β-pic	1579s	1479s	1414m	1190m	1229w	1126m	1044m
$SbCl_3$·β-pic	1548s	1471m	1385m	no	1256m	no	1116m
SbI_3·β-pic	1543s	1466m	1383m	no	no	1249m	no
γ-pic	1608s	1498w		1224m	802s	1224	727
$SbCl_3$·γ-pic	1562s	no	1385w	1254w	678s	1254	653
SbI_3·γ-pic	1634s	no	1384w	1241m	751s	1245	699

ν=stretch; δ=bending in-plan; ω=ring bending out-of-plane; β=bending out-of-plane; ϕ=ring bending in-plane; X-sens=C–CH_3; s=strong band; m=medium band and w=weak band

^1H and ^{13}C NMR

The chemical shift δ (ppm) and the assignment values for the corresponding ^1H and ^{13}C NMR signals for ligands and adducts are given in Table 3. The attribution of these signals was based on previous reports for ligands [13, 14] and for adducts [15–18]. For all adducts, ^1H signals were shifted to lower field when compared to those in the free ligands. The change of chemical shift in ^1H NMR of ligands before and after coordination ($\Delta\delta=\delta_{adduct}-\delta_{free\ ligant}$) were calculated to give a positive difference. This fact is a clear indication that occurs an electronic density decrease of ligands after coordination. In order to investigate the nature of element–picoline interaction, represented by Sb–Lpic, it was chosen the H_c proton as probe. This chosen was based on the fact that H_c proton was no affected by substituted effects as occurs with H_d, which signal depends on the attached group in ortho position. Basing on previous data [15] involving

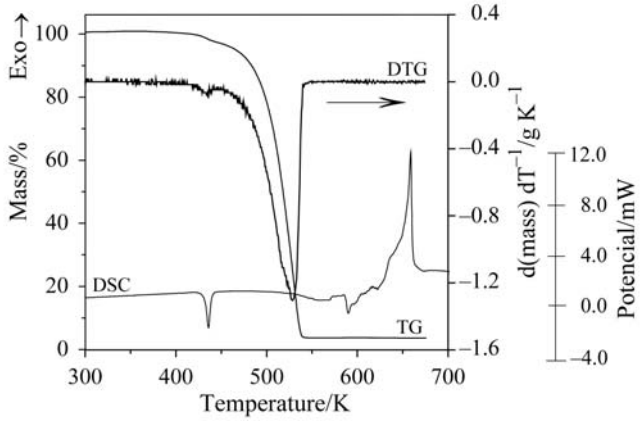

Fig. 2 TG, DTG and DSC data for SbI_3·α-pic adduct

Table 3 ^{1}H and ^{13}C NMR data for adducts and α-, β- and γ-picolines

Adducts	^{1}H					^{13}C					
	CH_3	H_c	H_b	H_a	H_d	CH_3	C_2	C_3	C_4	C_5	C_6
α-pic	2.54(s-3H)	7.16(t-H)	7.63(t-H)	7.20(d-H)	8.42(d-H)	24.45	158.34	123.54	136.22	120.66	149.10
$SbCl_3$·α-pic	2.70(s-3H)	7.69(t-H)	7.75(d-H)	8.26(t-H)	8.70(d-H)	20.80	154.86	126.38	143.14	123.36	143.43
SbI_3·α-pic	2.73(s-3H)	7.92(t-H)	7.98(d-H)	8.56(t-H)	8.83(d-H)	19.38	153.62	127.83	141.14	124.41	146.22
β-pic	2.30(s-3H)	7.25(t-H)	8.44(d-H)	7.58(d-H)	8.38(s-H)	18.41	150.25	133.07	136.40	123.12	146.98
$SbCl_3$·β-pic	2.51(s-3H)	7.82(t-2H)	8.74(s-H)	8.24(d-H)	8.64(d-H)	17.78	144.17	136.73	141.02	125.84	143.45
SbI_3·β-pic	2.73(s-3H)	8.02(t-H)	8.50(d-H)	8.78(d-H)	8.84(s-H)	17.84	147.04	138.08	139.14	126.73	141.31
γ-pic	2.33(s-3H)	8.40(d-H)	7.20(d-2H)	8.74(d-2H)	7.02(d-2H)	20.72	149.56	124.37	146.75	124.37	149.26
$SbCl_3$·γ-pic	2.51(s-3H)	8.69(d-H)	7.71(d-2H)	8.69(d-2H)	8.71(d-2H)	21.34	155.54	126.68	143.64	126.58	155.54
SbI_3·γ-pic	2.73(s-3H)	8.82(d-H)	8.82(d-2H)	7.96(d-2H)	7.96(d-2H)	21.18	160.09	127.93	140.93	127.93	160.09

s = singlet, d = doublet and t = triplet

pyridine (py) and its derivatives, it was observed a good correlation between $\Delta\delta_{adduct}$ (^{1}H) and the correspondent pKa of the protoned ligands, which results are an indicative of absence of bonding on (M→Lpy) interaction, in agreement with the importance of σ(Lpy→M) bonding, where *M* is a metallic atom without sharing electrons on bond formation [15]. Taking into account this information, some correlation was tested between pKa of picolines and $\Delta\delta_{adduct}$ (^1H_c) values for two series of adducts, without obtaining any correlation. Thus, $\Delta\delta_{adduct}$ (^1H_c) values for both series of adducts showed the sequence for proton chemical shift δ(α-pic)≅δ(β-pic)>δ(γ-pic). On the other hand, this fact does not imply that the π Sb–Y-pic bonding is present, which inferred that antimony non-ligand electrons were also shared by antiligand orbital of aromatic ring. For protons of methyl group, the signals in adducts were down field displaced in both series compared with the free ligand signals and for triiodide δ_{adduct} (^{1}H) values are located at high field.

For adducts ^{13}C NMR spectra the shifts were observed towards lower fields for carbon C_2 and C_6 atoms and at higher fields for C_3, C_4 and C_5 atoms. The methyl group signal values were displaced to higher field in SbX_3·α-pic adduct, whereas the same signal for other adducts shifted to lower field.

As a general behavior, ^{13}C resonance signals for free pyridinic ring and coordinated ligands with antimony, showed identical chemical shifts as observed for pyridinium cation. Chemical shift of ortho carbons changed to upfield and meta/para carbons signal for downfield with high chemical shift for para carbon. By considering the halogens, it was observed a high carbon chemical shift values for triiodides in both regions of up and downfield. This behavior is also observed for aromatic ring protons. With exception of methyl carbon signal in ortho position all other signals occur near zero chemical shift, indicated that methyl carbon was protected after coordination. This fact can be associated with carbon of methyl group is shielding by electronic density of halogen p orbital.

A correlation between δ($^{13}C_5$) signals of adducts and pKa values for the corresponded protoned picolines were tried without success. However, it was proposed the effect of antimony salt over chemical shift of aromatic carbons, given by the relationship: [Δ(Δδ)=(adduct–δligand)–(δligand–δpyridine)]. From these values a good correlation was obtained between Δ(Δδ) and pKa of picolines for two series of compounds with correlation coefficient (*r*) 0.9995 and 0.998 for trichloride and triiodide series, respectively. Based on Δδ for C_6, the sequence of shifts δ(α-pic)≅δ(γ-pic)<δ(β-pic) is observed for both series of adducts, which is the same pKa sequence values for protoned ligands.

By considering the same ligand forming adducts with trichloride and triiodide, the difference between carbon chemical shift values before and after coordination, it was not obtained a constant value for both series. This fact indicated that different paramagnetic contributions of chlorine and iodine atoms over carbon in each adduct. This behavior suggests that other effects beyond electronegativity and halogen size affect the chemical shifted of aromatic carbon.

These results obtained from ^{1}H and ^{13}C NMR spectra suggest that the bond between SbX_3 (*X*=halide) and the ligands Y-pic is formed by sharing the lone pair elec-

trons of nitrogen and the vacant sp^3d orbital of antimony in a general expected bipyramide trigonal structure.

Kinetic of thermal decomposition

The application of isothermal technique for decomposition study of adducts enabled the identification of the mechanism by which such reaction occurs and also the determination of kinetic parameters such as apparent activation energy (E) and frequency factor (A). The kinetic analysis was based on different models for thermal decomposition reactions in solid-state [19, 20].

Under isothermal conditions, the data of fractional reaction-time (α–t) were treated by applying linear regression in the form $g(\alpha)=kt+k_0$ where k and k_0 were constant and $g(\alpha)$ is the function depends on the mechanism controlling the reaction and on the size of the reacting particles. For the phase boundary controlled reactions, we have the contracting area or R_2 model, $g(\alpha)=1-(1-\alpha)^{1/2}$ and the controlled sphere or R_3 model $g(\alpha)=1-(1-\alpha)^{1/3}$. If the solid-state reaction is controlled by nucleation followed by growth, then in this case we may have the Avrami equation for initial nucleation followed by overlapping growth in two-dimensions, A_2 function, $g(\alpha)=[-\ln(1-\alpha)]^{1/2}$; the Erofeev equation for initial random nucleation followed by overlapping growth in three-dimensions, A_3 function, $g(\alpha)=[-\ln(1-\alpha)]^{1/3}$; and the Prout–Thomkis equation for branching nuclei, A_1 function, $g(\alpha)=\ln[\alpha/(1-\alpha)]$.

The choice of the temperature adopted to the accomplishment of the experiment was made with the help of the thermogravimetric dynamic curves, by using a heating rate of $8.25\cdot10^{-2}$ K s^{-1} as illustrated by Fig. 2.

Adjustments were performed for decomposition values function, $\alpha>0.15$, because with lower values the experiment did not present isothermal characteristics. Using an interval $0.15<\alpha<0.95$, and on the basis of reduced time method and ln.ln, of the best adjustment of coefficient of linear correlation and the standard deviation the models R_1 and A_4 for $SbCl_3\cdot L$ adducts and R_1 and A_2 for $SbI_3\cdot L$ adducts presented better results. The reduced time method ($t_r=t/t_{0.5}$) as well as ln.ln method enabled to distinguish among the three processes the decomposition in solid state, such as nucleation and increasing, diffusion and boundary phase. The obtained kinetic parameters for the respective series of adducts are listed in Tables 3, 4 and 5. Both calculation methods for $SbCl_3\cdot\alpha$-pic and $SbI_3\cdot\alpha$-pic adducts are shown in Figs 3 and 4, respectively. By comparing the theoretical and the experimental curves for these results, it was possible to define with high precision the most appropriated model for these decomposition processes for the adducts.

The parameter k_0 for the rate equation was approximately equal to naught in every fitting, which justified by the fact that the experimental curve, which demonstrate practically that the induction period did not appeared in the beginning of decomposition.

Table 4 Rate constant (k), linear correlation coefficient (r) and standard deviation (s) for thermal decomposition of $SbCl_3$·α-pic adduct by using R1 model

Model	Parameter	Temperature of the isotherm/K					
		393	398	408	413	418	423
R_1	k/s^{-1}	$4.52\cdot10^{-5}$	$5.94\cdot10^{-5}$	$1.17\cdot10^{-4}$	$1.59\cdot10^{-4}$	$2.01\cdot10^{-4}$	$2.98\cdot10^{-4}$
	r	0.9999	0.9999	0.9999	0.9999	0.9998	0.9998
	s	$2.90\cdot10^{-3}$	$1.17\cdot10^{-3}$	$2.73\cdot10^{-3}$	$2.96\cdot10^{-3}$	$3.83\cdot10^{-3}$	$4.29\cdot10^{-3}$
A_4	k/s^{-1}	$3.30\cdot10^{-5}$	$4.34\cdot10^{-5}$	$8.55\cdot10^{-5}$	$1.16\cdot10^{-4}$	$1.47\cdot10^{-4}$	$2.18\cdot10^{-4}$
	r	0.9988	0.9988	0.9992	0.9992	0.9989	0.9983
	s	$7.89\cdot10^{-3}$	$7.76\cdot10^{-3}$	$6.48\cdot10^{-3}$	$6.46\cdot10^{-3}$	$7.45\cdot10^{-3}$	$9.31\cdot10^{-3}$

Table 5 Rate constant (k), linear correlation coefficients (r) and standard deviation (s) for thermal decomposition of $SbCl_3$·β-pic adduct

Model	Parameter	Temperature of the isotherm/K					
		398	404	404	410	413	416
R_1	k/s^{-1}	$5.96\cdot10^{-5}$	$9.33\cdot10^{-5}$	$1.14\cdot10^{-4}$	$1.36\cdot10^{-4}$	$1.60\cdot10^{-4}$	$1.92\cdot10^{-4}$
	r	0.9981	0.9999	0.9999	0.9999	0.9999	0.9999
	s	$1.35\cdot10^{-2}$	$2.31\cdot10^{-3}$	$2.83\cdot10^{-3}$	$2.76\cdot10^{-3}$	$2.84\cdot10^{-3}$	$3.47\cdot10^{-3}$
A_4	k/s^{-1}	$4.35\cdot10^{-5}$	$6.82\cdot10^{-5}$	$8.31\cdot10^{-5}$	$9.97\cdot10^{-5}$	$1.17\cdot10^{-4}$	$1.4\cdot10^{-4}$
	r	0.9971	0.9991	0.9991	0.9991	0.9992	0.9991
	s	$1.89\cdot10^{-2}$	$6.87\cdot10^{-3}$	$6.93\cdot10^{-3}$	$6.73\cdot10^{-3}$	$6.44\cdot10^{-3}$	$6.93\cdot10^{-3}$

Table 6 Rate constants (k), linear correlation coefficients (r) and standard deviation (s) for thermal decomposition of the adduct $SbCl_3$·γ-picoline

Model	Parameter	Temperature of the isotherm/K					
		413	417	421	425	429	433
R_1	k/s^{-1}	$8.43\cdot10^{-5}$	$1.14\cdot10^{-4}$	$1.49\cdot10^{-4}$	$1.20\cdot10^{-4}$	$2.46\cdot10^{-4}$	$3.09\cdot10^{-4}$
	r	0.9996	0.9999	0.9998	0.9999	0.9999	0.9995
	s	$6.34\cdot10^{-3}$	$3.59\cdot10^{-3}$	$4.48\cdot10^{-3}$	$2.23\cdot10^{-3}$	$2.09\cdot10^{-3}$	$6.80\cdot10^{-3}$
A_4	k/s^{-1}	$6.12\cdot10^{-5}$	$8.33\cdot10^{-5}$	$1.09\cdot10^{-4}$	$1.46\cdot10^{-4}$	$1.80\cdot10^{-4}$	$2.26\cdot10^{-4}$
	r	0.9988	0.9992	0.9994	0.9999	0.9989	0.9986
	s	$7.85\cdot10^{-3}$	$6.31\cdot10^{-3}$	$5.77\cdot10^{-3}$	$7.56\cdot10^{-3}$	$7.33\cdot10^{-3}$	$8.51\cdot10^{-3}$

The thermal decomposition results for all adducts are listed in Table 7. By comparing the kinetic parameter from Table 7 with that one obtained by other models, it was observed that the values of the kinetic parameters are independent on the applied model used for kinetic data determination as it was demonstrated by many other sys-

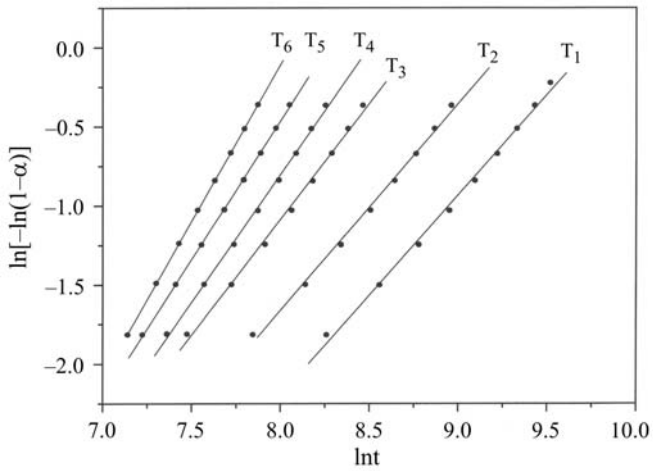

Fig. 3 Application of ln.ln analytical method for SbI_3·α-pic adduct with T_1=418, T_2=423, T_3=433, T_4=438, T_5=433, T_6=448 K and values of Z=1.24; 2.00; 4.00; 1.55 for R_1, A_2, A_3, A_4 models and experimental, respectively

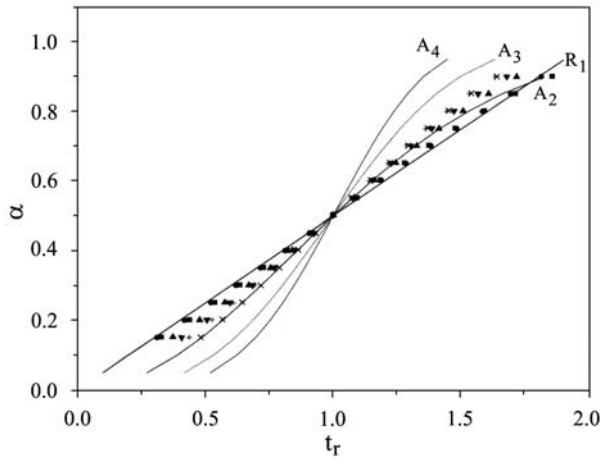

Fig. 4 Application of boundary time method (t_r) for SbI_3·α-pic adduct at ● – 418, ■ – 423, ▲ – 433, ▼ – 438, + – 433, × – 448 K and R_1, A_2, A_3, A_4 theoretical curves

tems [21]. In present case, the activation energy of decomposition for adducts obtained through isothermal process, showed the sequence of stability:

i) $SbCl_3$·α-pic<$SbCl_3$·β-pic<$SbCl_3$·γ-pic and *ii*) SbI_3·β-pic<SbI_3·γ-pic<SbI_3·α-pic.

Table 7 Enthalpy of activation (E), frequency factor (A) and coefficient of correlation (r) for the kinetic parameters derived from isothermal thermogravimetric data for application of Arrhenius law using R_1 and A_2 models for all adducts

	Model R_1			Model A_2		
Adducts	E/kJ mol^{-1}	A/s^{-1}	r	E/kJ mol^{-1}	A/s^{-1}	r
$SbCl_3$·α-pic	86.68	$1.42\cdot10^7$	0.9988	–	–	–
$SbCl_3$·β-pic	88.95	$2.65\cdot10^7$	0.9985	–	–	–
$SbCl_3$·γ-pic	96.70	$1.47\cdot10^8$	0.9986	–	–	–
SbI_3·α-pic	94.00	$2.54\cdot10^7$	0.9954	94.06	$3.54\cdot10^7$	0.9954
SbI_3·β-pic	88.00	$4.79\cdot10^6$	0.9983	89.00	$5.87\cdot10^6$	0.9984
SbI_3·γ-pic	90.00	$4.70\cdot10^6$	0.9991	90.00	$6.63\cdot10^6$	0.9993

The apparent controversy related to the application of isothermal and non-isothermal techniques for study of decomposition of solids and also the proposed suggestions presented by Blecic [22], led us to the application of the dynamic thermogravimetric curves by using integral methods. The conclusion is that for a total analysis, both techniques should be used for such proposal. The integral methods are habitually the favorite one because they do not present the disadvantage of data dispersion that frequently hinders or disables the use of the differentiate methods [23–25]. However, when applied for a given system, it should be used with caution, because almost always enable to find a series of kinetic parameters (A, E and n), which could be adapted to the experimental data, and these parameters contribute to the understanding of the mechanism of the studied reaction [10].

A plot of ln$k$ *vs.* T^{-1} allows the determination of the activation energy values and frequency factor by using the angular and linear coefficients, respectively, as illustrated in Fig. 5. The kinetic activation energy (E) parameters and the frequency factor (A) were obtained by Arrhenius equation with rate constants, k, relative to R_1 model, as an example, it was applied for $SbCl_3$·γ-pic and SbI_3·γ-pic adducts, as shown in the Fig. 5.

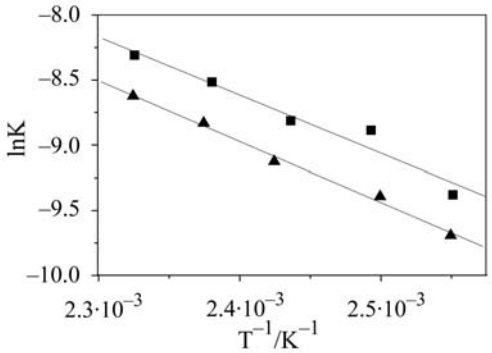

Fig. 5 Application of Arrhenius equation relative to –■– – R_1 and A_4 –▲– models applied for $SbCl_3$·β-pic adduct

The method of Coats–Redfern [10] was used for ϕ=0.167 K s^{-1}, then, with the substitution of the functions $g(\alpha)$ to give

$$\ln\left[\frac{g(\alpha)}{T^2}\right]=\ln\left[\frac{AR}{\phi E}\right]-\frac{E}{RT}$$

where T is the absolute temperature, R the gas constant in kJ K^{-1} mol^{-1}, universal of ideal gases, ϕ the rate of heating (K s^{-1}), A the frequency factor in s^{-1}, E the energy of activation in kJ mol^{-1} and $g(\alpha)$ the functions corresponded to Avrami–Erofeev and the boundary phase, models used for analyzing the obtained data, by using isothermal method.

Table 8 Kinetic parameters derived from non-isothermal thermogravimetry for application of the function $g(\alpha)$ in the Coats–Redfern equation using the R_1 and R_2 models for adducts

	Model R_1			Model R_2		
Adducts	E_a/kJ mol^{-1}	A/s^{-1}	r	E_a/kJ mol^{-1}	A/s^{-1}	r
$SbCl_3$·α-pic	76.45	$7.68\cdot10^5$	0.9992	94.41	$2.73\cdot10^7$	0.9997
$SbCl_3$·β-pic	81.57	$2.74\cdot10^6$	0.9965	96.81	$1.01\cdot10^8$	0.9965
$SbCl_3$·γ-pic	92.28	$3.54\cdot10^7$	0.9997	109.86	$4.28\cdot10^9$	0.9986
SbI_3·α-pic	86.90	$3.19\cdot10^6$	0.9998	103.64	$1.39\cdot10^8$	0.9983
SbI_3·β-pic	83.28	$9.53\cdot10^5$	0.9959	101.08	$5.28\cdot10^7$	0.9995
SbI_3·γ-pic	86.25	$2.06\cdot10^6$	0.9997	103.26	$9.23\cdot10^7$	0.9976

In spite of the easiest application of the non-isothermal methods in comparison to the isothermal, this last one presents more reliable results, which is also used as reference in relation to parameters obtained through dynamic method. However, in agreement with Dollimore [26], the results could not be necessary in agreement from both isothermal and non-isothermal methods, taking into account the kinetic parameters and also the mechanism of decomposition. The results by applying the non-isothermal model are listed in Tables 8 and 9, which are in agreement with those observed by isothermal method, as presented in Table 5. On the other hand, it could be very difficult to identify the model used for this last method, without confronting the results with the isothermal one. The stability order in relation to the activation energy, by considering the non-isothermal process is:

i) $SbCl_3$·α-pic<$SbCl_3$·β-pic<$SbCl_3$·γ-pic and *ii*) SbI_3·β-pic<SbI_3·α-pic≅SbI_3·γ-pic.

This last sequence is the same of that one observed for pKa ligand values [15] and for the variation in chemical shift $\Delta(\Delta\delta)$ for carbon 6 of the aromatic ring.

In attempting to verify if another factor can influence the kinetic of reaction, other correlation involving the kinetic parameters E and A were used, which were determined from R_1 model, through the expression $\ln A=aE+b$, where a and b are constant. This equation represents the kinetic effect compensation. Thus, considering the kinetic parameter related to all adducts, which gave some interesting features related

to compensation kinetic. As example, for trichloride adducts and R_1 model, the parameters *E* and *A* are correlated. The values obtained for constants *a* and *b*, relative to the isothermal and non-isothermal methods, were 0.23 and –3.44; 0.24 and –4.90, respectively, corresponding to the correlation coefficients 0.999 and 1.000. However, for triiodide adducts, the relationship between *A* and *E* differs, showing a correlation coefficient of 0.985. The observed effect for kinetic compensation for trichloride adducts can be related to many factors such as the binding energy of antimony–ligand, impurities, whose functions are not appropriated as a kinetic model, and so on.

Conclusions

The two characterized series of adducts of the type SbX_3·L-pic (*L-pic*=2-, 3- and 4-picolines, *X*=Cl and I) showed ^1H and ^{13}C NMR signals for triiodide adducts at much higher fields than analogous trichloride adducts. The absence of correlation between the variation of chemical shifts of H_c protons for the adducts and the correspondent pKa values for the protonated ligands implies that in the (Sb–Lpic) bond, beyond the participation it could be used π contribution. Therefore, by using δC_4 as a valid probe to inform about π bond, which could be important in metal–ligand bond formation as observed for platinum complexes [15, 28], where such high field chemical shift is in the order of 4.5 ppm. In the present case, a change for down field varying from 0.33 to 13 ppm was observed. From these results it was concluded that in agreement with δC_4 values found for both series of adducts, the participation of π bond should be absent in the Sb–Lpy bond.

R_1 model presented the best adjusting for experimental data obtained by isothermal and non-isothermal processes. An agreement for activation energies determined for two processes using such model was obtained. The proposed sequence with the activation energies for triiodide adducts, obtained through non-isothermal process, as well that established for δC_6 values for the same adducts are in agreement with pKa values for protonated ligands and also the maintenance of the same order.

* * *

The authors thank to CAPES, CNPq and PADCT for financial support.

References

1 G. Liptay, G. Kenessey, L. Bihátsi, T. Wadsen and J. Mink, J. Thermal Anal., 38 (1992).
2 G. Liptay, G. Kenessey and J. Mink, Thermochim. Acta, 214 (1993) 71.
3 F. A. Mautner and M. A. S. Goher, Polyhedron, 12 (1993) 2823.
4 N. Sultana, H. Tabassum and M. S. Arayne, Indian J. Chem. A, 33 (1994) 63.
5 F. A. Mautner and M. A. S. Goher, Polyhedron, 11 (1992) 2537.
6 L. O. P. Dustan, Thermochim. Acta, 345 (1986) 456.
7 B. Ptaszynski, Thermochim. Acta, 232 (1994) 137.
8 L. C. R. Santos, J. Q. Caluęte and A. G. Souza, Thermochim. Acta, 292 (1997) 71.
9 L. C. R. Santos, J. G. P. Espínola and A. G. Souza, Thermochim. Acta, 241 (1994) 17.

10 A. W. Coats and J. P. Redfern, Nature, 201 (1964) 68.
11 J. H. S. Green, W. Kynaston and H. M. Paisley, Spectrochim. Acta, 19 (1963) 54.
12 O. P. Lamba, J. S. Parihar and Y. S. Jaint, Indian J. Pure Appl. Phys., 21 (1983) 236.
13 F. Scheinmann, An Introduction to Spectroscopic Methods for the Identification of Organic Compound, Vol. 1, Pergamon Press 1970.
14 E. Breitmaier and W. Voelter, ^{3}C NMR Spectroscopy – Methods and Applications in Organic Chemistry, 2nd edition, Verlaz Chemie-Weinhein, New York 1978.
15 C. Tessier and F. D. Rochon, Inorg. Chim. Acta, 295 (1999) 25.
16 T. M. Klapotke and T. Schutt, J. Fluorine Chem., 109 (2001) 151.
17 A. V. Ivanov, V. I. Mitrofanova, M. Kritikos and O. N. Antzutkin, Polyhedron, 18 (1999) 2069.
18 A. V. Ivanov, T. Rodyna and O. N Antzutkin., Polyhedron, 17 (1998) 3101.
19 M. E. Brown, D. Dollimore and A. K. Galwey, Comprehensive Chemical Kinetics, Vol. 22, Elsevier, Amsterdam 1980.
20 A. M. M. Gadalla, Thermochim. Acta, 74 (1984) 255.
21 J. M. Criado, M Gonzales, A. Ortega and C. Real, J. Thermal Anal., 29 (1984) 24350.
22 D. Blecic, Ž. D. Živkovic and M. Martinovic, Thermochim. Acta, 60 (1983) 234.
23 T. Ozawa, J. Thermal Anal., 2 (1970) 301.
24 G. G. Mohamed and Z. H. Abd El-Wahab, J. Therm. Anal. Cal., 73 (2003) 347.
25 H. Arslan, J. Therm. Anal. Cal., 66 (2002) 399.
26 J. Zsakó, J. Thermal Anal., 5 (1973) 239.
27 D. Dollimore, Anal. Chem., 62 (1990) 15.
28 D. K. Lavallee, M. D. Baughman and M. P. Phillips, J. Am. Chem. Soc., 99 (1977) 718.